The use of chirped fibre Bragg grating sensors to monitor delaminations in composite materials and structures

S. L. Ogin, A. D. Crocombe, T. F. Capell, A. R. Sanderson, R. L. Rito
Faculty of Engineering and Physical Sciences, University of Surrey, Guildford, UK

Yalin Guo
Xi'an Aerospace Composites Research Institute, Xi'an, Shaanxi, P. R. China

S. C. Tjin, B. Lin
School of Electrical and Electronic Engineering, Photonics Research Centre, Nanyang Technological University, Singapore

ABSTRACT: Chirped fibre Bragg grating (CFBG) sensors embedded within composite materials have been shown to be able to monitor delamination growth in adhesively bonded single-lap joints, whether the sensors are embedded within a composite adherend or within the adhesive bondline itself. The relative ease of interpretation of CFBG reflected spectra with regard to delamination growth is a consequence of the relationship between the spectral bandwidth of the reflected spectrum (typically 20 nm) and physical locations along the sensor length (typically 60 mm). When the sensor is embedded in, or bonded to, a composite material subjected to a tensile uniform strain, all the grating spacings are increased and the entire spectrum shifts to higher wavelengths – just as for a uniform FBG sensor. However, if the strain field is perturbed by damage in the composite (such as a matrix crack or a delamination), so that the smooth linear increase in the grating spacing is disrupted, then a perturbation appears in the reflected spectrum that can be used to determine the physical location of the damage. In this paper, results on monitoring delamination/disbond growth will be discussed with regard to sensor location, together with the possibility of using the sensors to monitor repaired composite structures.

1 INTRODUCTION

Fibre Bragg grating (FBG) sensors have been in use for many years to monitor strain or temperature changes. The basic principle of operation is simple, in that a periodic variation of the refractive index introduced within the core of an optical fibre reflects light with a wavelength, the Bragg wavelength, λ_B (Figure 1), where λ_B is related to the grating spacing, Λ, and the effective refractive index, n_{eff}, by

$$\lambda_B = 2n_{eff}\Lambda$$

In essence, then, when the grating spacing changes, as a consequence of strain or temperature, the reflected wavelength, λ_B, from an input broadband light source (i.e. a light source having an approximately uniform intensity over a range of wavelengths) changes. The strain sensitivity is typically approximately 1.2 x 10^{-3} nm/με. For a chirped FBG sensor, on the other hand, the grating spacing changes uniformly along the sensor length. Consequently, provided the local density of grating spacings is constant, a spectral bandwidth is reflected with uniform intensity. In Figure 1, the 20 nm spectral bandwidth corresponds to the 60 mm sensor length.

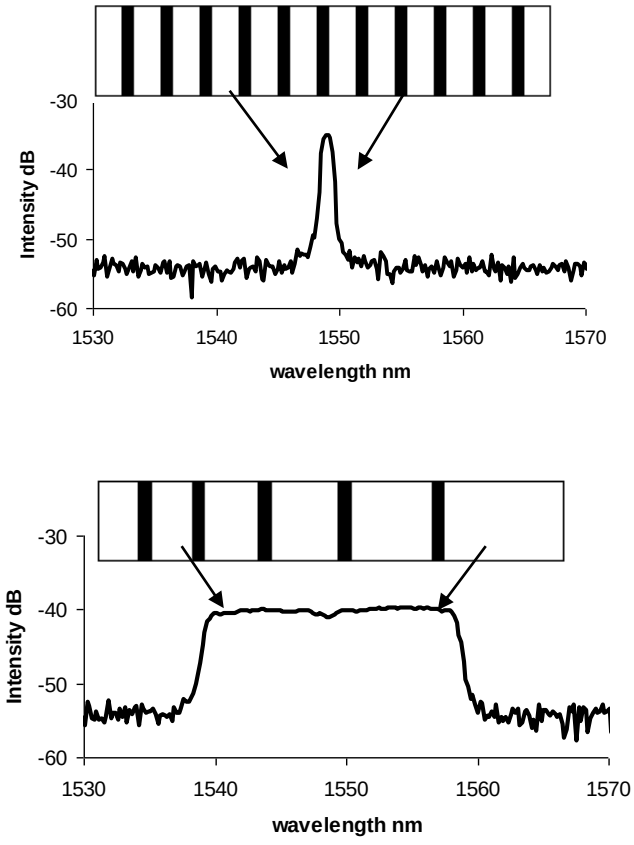

Figure 1. Fibre Bragg gratings: uniform grating spacing (above); chirped fibre Bragg grating (below).

Takeda and colleagues (e.g. Okabe et al, 2004) appear to have been the first to use chirped FBG (CFBG) sensors to detect damage in composite materials. For CFBGs, a *uniform* strain applied parallel to the length of the sensor gives rise to a shift of the entire spectrum (as all the grating spacings change in response to the strain), but a *non-uniform* local strain caused by damage alters the local density of the grating spacings, and the resulting perturbation in the reflected spectrum identifies the damage location. By embedding a CFBG sensor in the 0^0 ply of a cross-ply CFRP laminate close to the 0/90 interface, Okabe and colleagues were able to identify the position of individual matrix cracks in the 90^0 ply which developed when the coupons were loaded. Load-shedding around the 90^0 ply cracks into the 0^0 ply caused local perturbations to the strain field which modified the local grating spacing, giving rise to changes in the reflected intensity corresponding to the crack locations.

The capability of the CFBG sensor to locate perturbations in the strain field caused by damage within composite materials has been extended to the detection of delamination/disbonding of bonded composite joints.

2 DISBONDING OF BONDED JOINTS: SENSOR EMBEDDED WITHIN ONE ADHEREND – IDENTICAL ADHERENDS

The disbonding, or delamination, of a bonded composite joint can be readily monitored using a CFBG sensor embedded within one adherend (Palaniappan et al. 2005; 2008). Figure 2 shows a schematic of two GFRP adherends bonded together, over a 60 mm length, to form a single-lap joint. The transparent GFRP coupons both have a lay-up $(0_2/90/0_6)_s$ and dimensions 120 x 20 x 4.5 mm, with the CFBG sensor embedded within the outer 0^0 ply, near the 0/90 interface.

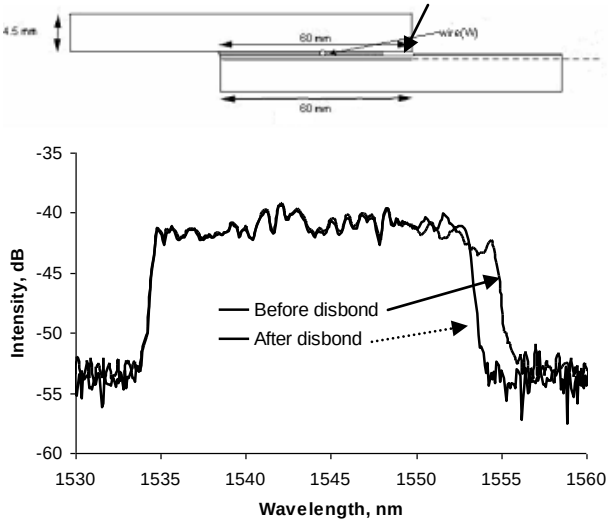

Figure 2. Detection of disbond initiation due to relation of grating spacings in the disbonded region of a single-lap joint.

The bonded joint was subjected to fatigue loading which initiated disbonding of the joint. Figure 2 shows the reflected spectra before and after disbonding initiated - in both cases when the bonded joint was subjected to a small tensile load. In this example, the initiating disbond was adjacent to the high-wavelength end of the sensor. When the delamination/disbond initiates, load is no longer carried close to the end of the adherend adjacent to the disbond, which in this case was also the adherend within which the sensor was located. Since this region is now unloaded, the grating spacings relax here, and the high-wavelength end of the reflected spectrum moves to lower wavelengths. In other words, disbond initiation can be detected.

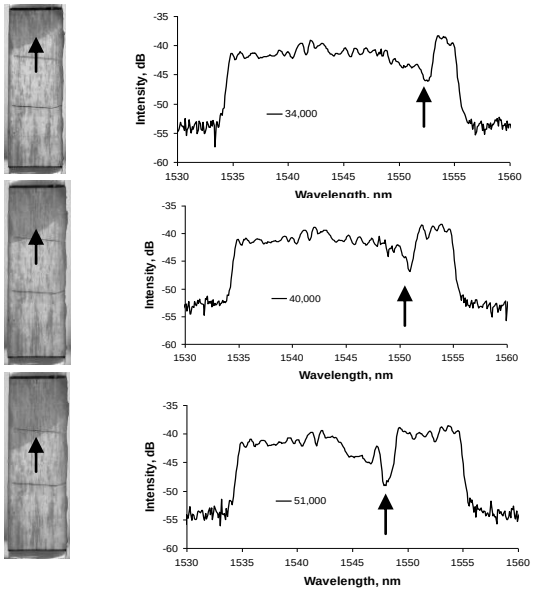

Figure 3. Detection of disbond growth using a sensor embedded within one adherend for increasing numbers of fatigue cycles.

Figure 3 shows how disbond growth due to fatigue loading of the joint can also be monitored. The growth of the disbond can be seen in Figure 3 as an extension of the shaded region within the 60 mm long overlap length of the joint; the progression of the disbond can be seen because both GFRP adherends are transparent. As the disbond grows, the position of the disbond front appears in the reflected spectrum which progresses to lower wavelengths as the disbond extends (note: the fatigue test had to be interrupted and the joint put under a small quasi-static tensile load, in order to record the spectra in this case). As before, the perturbation within the reflected spectrum is due to the load transfer between the two adherends at the disbond front. The adherend with the embedded sensor takes an enhanced load (and hence, strain) at the position of the disbond front; this enhanced strain locally increases the grating spacing. The consequence is a local dip in the spectrum (since the reflected intensity is a function of the local density of the grating spacings) and an increase of the

intensity at higher wavelengths, as the increased grating spacings add to the grating spacings already present towards the higher wavelength end of the sensor. Finite-element analysis to predict the strain distribution along the sensor length, and subsequent use of the commercial software OptiGrating, enabled a prediction of the expected reflected spectrum to be made which was in very good agrement with the experimental results (Palaniappan et al. 2008).

In this example, the adhesive used to produce the bonded joint was cured well above room temperature (at 120^0 C), but since the GFRP adherends were identical, no thermal strain mismatch occurs between the adherends. For the case of adherends with disimilar coefficients of thermal expansion which are also bonded at elevated temperature, thermal mismatch strains develop between the adherends. With the aid of the CFBG sensor, the relaxation of these thermal mismatch strains can be used to monitor disbond initiation and growth without the need to load the joint mechanically.

3 DISBONDING OF BONDED JOINTS: SENSOR EMBEDDED WITHIN ONE ADHEREND – DISIMILAR ADHERENDS

Figure 4 shows a schematic diagram of a joint manufactured using one GFRP adherend, of the type discussed above, bonded at 120^0 C to an aluminium adherend. Again, the CFBG sensor was embedded in the GFRP adherend at the 0/90 interface closest to the adhesive bondline. The high-wavelength end of the sensor was located towards the end of the GFRP adherend (Capell et al. 2007).

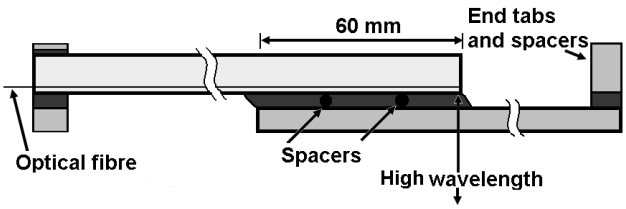

Figure 4. Schematic of a GFRP adherend (above) bonded to an aluminium adherend (below).

The coefficients of thermal expansion (CTEs) and Young's moduli in the loading direction of the GFRP adherend and the aluminium were about 7.5 x 10^{-6} K^{-1} and 40 GPa (GFRP), and 23.5 x 10^{-6} K^{-1} and 69 GPa (aluminium). As a result, there was a compressive residual thermal strain within the GFRP adherend (after bonding at 120^0 C and cooling to room temperature) of about 1100 με. Consequently, when a disbond initiated, this locked-in thermal strain was relaxed and the CFBG sensor gratings within the relaxed portion of the embedded sensor increased in length. This effect is shown schematically in Figure 5.

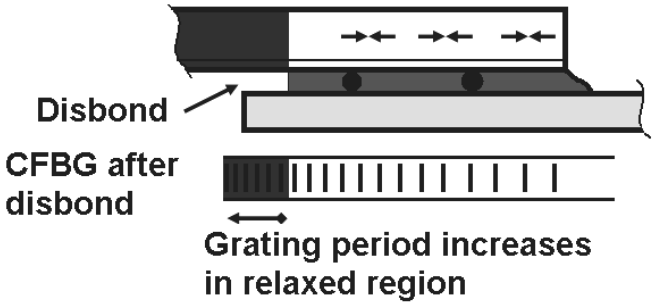

Figure 5. Relaxation and increase of grating spacings within that part of the CFBG sensor within the disbonded part of the adherend.

There is now an increased number of gratings with the same grating spacings ahead of, and behind, the disbond front. Consequently, a perturbation consisting of enhanced reflected intensity is seen in the reflected spectra corresponding to the position of the disbond front (Figure 6). The perturbation progressed from the low- to the high-wavelength end of the reflected spectrum as the disbond grew. As indicated above, what is noteworthy in this case is that the perturbation is caused by the realxation of thermal mismatch strain between the adherends, and no external load is required for the disbond front position to be located. This is true for any adherends with different CTEs bonded at an elevated temperature. In addition, if a room-temperature curing adhesive is used to bond adherends with different CTEs, raising (or lowering) the temperature of the joint should also enable the position of a disbond to be located, provided the thermal mismatch strains are large enough.

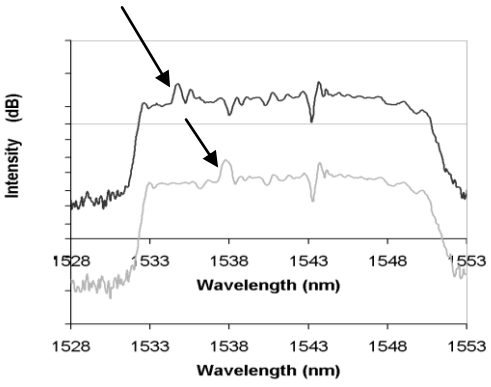

Figure 6. Progression of the perturbation as the disbond front grows along a specimen consisting of two adherends with different CTEs bonded at an elevated temperature. Note that the perturbations at 1548 nm and 1543 nm in the upper reflected spectrum are due to the wire spacers used to maintain a constant adhesive layer thickness.

4 DISBONDING OF BONDED JOINTS: SENSOR EMBEDDED WITHIN THE ADHESIVE BONDLINE

The previous sections illustrated the detection of a disbond using sensors embedded in one of the composite adherends. However, in some circumstances, it may not be possible to embed the sensor within an adherend - for example, when a concrete or metallic beam is reinforced with a plate-bonded composite reinforcement. In such cases, it may be necessary to locate the sensor within the adhesive bondline itself (Guo et al., to be published).

Figure 7 shows a schematic of a CFRP coupon (2.5 mm thick) bonded to a GFRP coupon (3 mm thick) as a single-lap joint, with the sensor embedded within the adhesive bondline (0.125 mm thick).

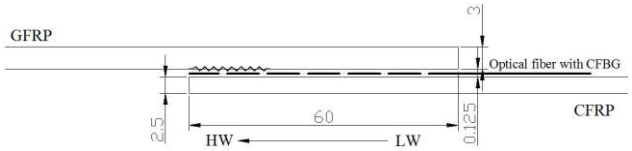

Figure 7. Schematic of a GFRP adherend bonded to a CFRP adherend, with a CFBG sensor embedded within the adhesive bondline; a disbond is shown propagating at the GFRP/adhesive interface adjacent to the HW end of the sensor.

In this case, the CTEs of the CFRP and GFRP adherends were estimated to be 0.26 x 10^{-6} K^{-1} and 9.7 x 10^{-6} K^{-1}, respectively, giving a CTE of the overlap length of the single-lap joint of approximately 2.9 x 10^{-6} K^{-1}. As before, the adhesive was cured at an elevated temperature. Taking the CTE of the optical fibre to be 0.5 x 10^{-6} K^{-1}, there is again a locked-in compressive thermal strain experienced by the sensor when the joint cools from the adhesive curing "lock-on" temperature to room temperature, this time of about 200 με.

Figure 8 shows the development of the disbond in the 60 mm bonded length of the joint after 100,000, 116,000 and 124,000 fatigue cycles. The disbond was photographed through the transparent GFRP adherend, and some matrix cracking can be seen to have developed in the cross-ply GFRP adherend (this cracking is of no significance for the test since the 90^0 plies are within the adherend, not at the surface). Although the reflected spectrum for this sensor is quite noisy, the progression of the disbond is clearly shown by a sharp dip in the spectra which shifts progressively from high- to low-wavelength as the disbond grows. Observations of the fracture surface showed that the sensor remained bonded to the CFRP adherend as the disbond propagated. Within the disbonded region, the locked-in compressive thermal strain in the CFRP adherend (as a consequence of bonding at elevated temperature) relaxed. Consequently, the grating spacings of the sensor (which remained bonded to the CFRP adherend) relaxed, resulting in a local reduction in grating spacings and a perturbation in the form of a dip within the spectrum at the position of the disbond front (see Figure 8). The progression of the disbond can again be monitored with the joint is unloaded.

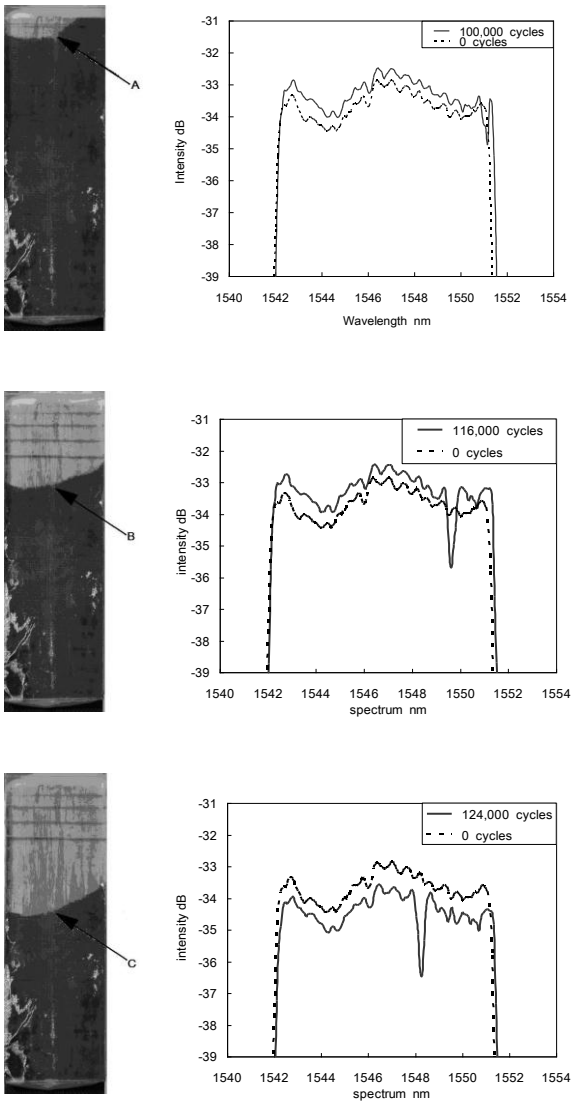

Figure 8. Observations of disbond growth in a GFRP/CFRP single-lap joint in fatigue, after 100,000, 116,000 and 124,000 cycles. The associated spectra from the CFBG sensor show a dip corresponding to the location of the disbond front.

5 DISBONDING OF BONDED JOINTS: SENSOR BONDED TO THE SPECIMEN SURFACE

In adition to sensors embedded within an adherend, or located within the adhesive bond line, a third possibility is for a sensor to be bonded to the surface of the structure of interest. This might be useful if the behaviour of ply-drops in fatigue is being monitored, for example. A demonstration of surface bonding is shown in the example of CFBG sensors

used to monitor delamination growth in a unidirectionally reinforced double-cantilever beam (DCB) specimen (Sanderson et al. 2011).

Figure 9 shows a schematic of a chirped CFBG sensor, with a 60 mm sensor length, surface-bonded to a unidirectionally reinforced transparent GFRP coupon tested as a DCB specimen. The insert shows an image of the specimen with the disbond front indicated with an arrow.

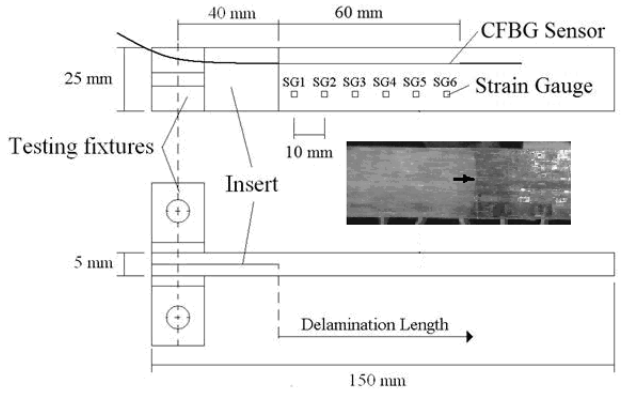

Figure 9. A surface-bonded CFBG sensor used to monitor delamination propagation in a DCB specimen. SG1 to SG6 are surface-bonded strain gauges for complementary measurements. The inset shows a specimen with the disbond front position indicated by an arrow.

The surface strains on the surface of a DCB specimen are compressive, reaching a maximum near the delamination front. Figure 10 shows the surface strains 30 mm either side of the delamination front as determined by surface bonded 1 mm gauge
tribution is
l colleagues
y reinforced
imen (using
edded close

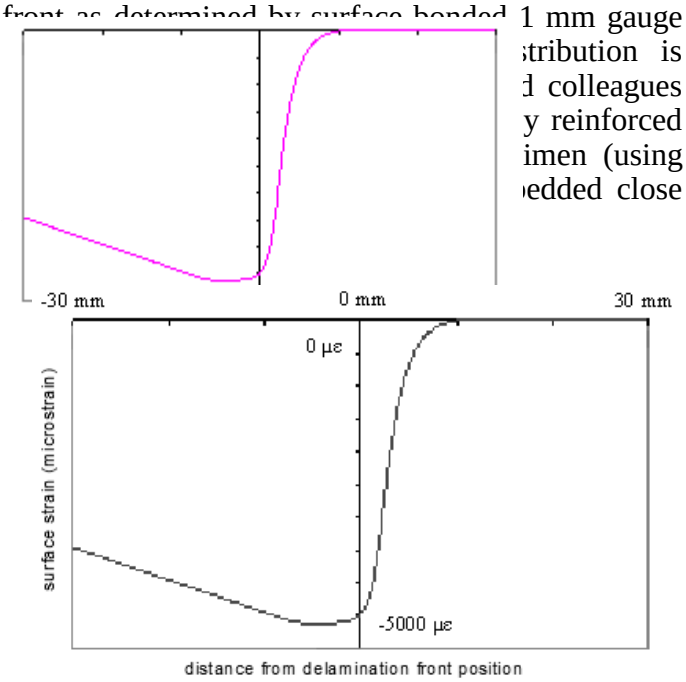

Figure 10. The surface strain distribution 30 mm either side of the delamination front in a DCB specimen, as determined with surface-bonded strain gauges.

An example of reflected spectra from a surface-bonded CFBG sesnsor for two delamination lengths is shown in Figure 11. A combination of finite-element analysis (to determine the surface strain distribution) and prediction of the resulting reflected spectra (using the commercial software OptiGrating), enabled the location of the disbond front to be determined, indicated by the arrows in the figure.

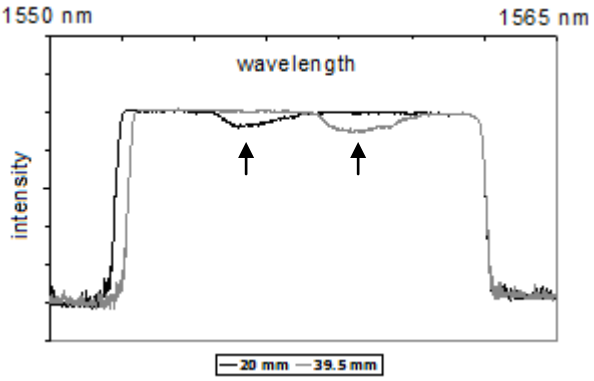

Figure 11. Reflected spectra for a DCB specimen at two delamination lengths. The arrows indicate the approximate delamination front positions in each case.

Figure 12 shows delamination lengths determined using surface-bonded CFBG sensor compared to delamination lengths measured using *in situ* photographs of the type shown in Figure 9. There is a good agreement between the two measurements.

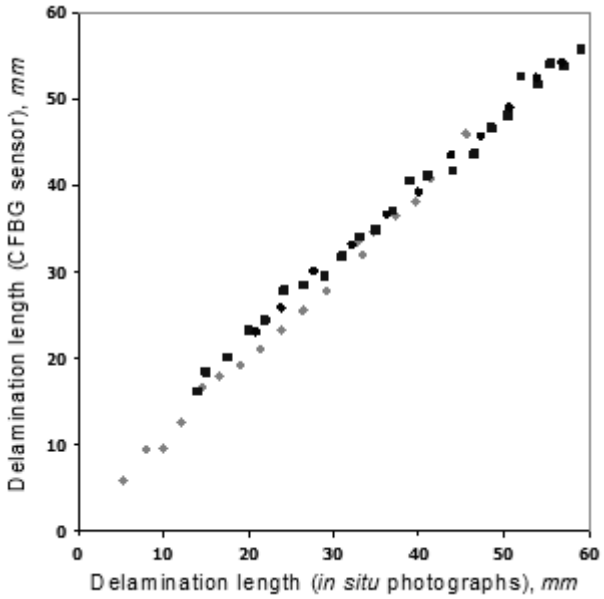

Figure 12. Comparison between delamination lengths determined using surface-bonded CFBG sesnsors and *in situ* photographs.

6 DETECTION OF FATIGUE DAMAGE ASSOCIATED WITH A SCARF REPAIR

A further example of the use of CFBG sensors to monitor delaminations is their potential use for monitoring fatigue damage associated with scarf-repaired damage in composite panels (Rito et al. 2011). Under flexural fatigue loading, it has been shown that a scarf repair in a model GFRP composite panel subjected to flexural fatigue loading

can develop fatigue cracks at the scarf repair/parent panel interface (Figure 13).

Figure 13. Development of a fatigue crack in a scarf-repaired composite panel subjected to flexural fatigue loading.

The fatigue cracks modify the near-surface strains in the vicinity of the interface between the repair and the parent panel (indicated schematically in Figure 12 by the modified path of the lines of force). A CFBG sensor, embedded between the parent panel and the overply used in the repair, detected both the initiation and propagation of this fatigue damage. First, when the fatigue crack initiated, the overply and the CFBG sensor fractured at the scarf repair/parent panel interface, causing the spectral bandwidth of the reflected spectrum to be significantly reduced (since reflections were prevented from those parts of the sensor beyond the fracture). Second, during crack propagation, the redistribution of near-surface strains due to stress-shielding by the growing fatigue crack caused changes to the reflected spectra. Figure 14 shows an example of the predicted change in the reflected spectrum for a fatigue crack which has grown to a length of about 5 mm at the scarf repair/parent panel interface. The experimentally recorded spectra were in good qualitative agreement with such predictions.

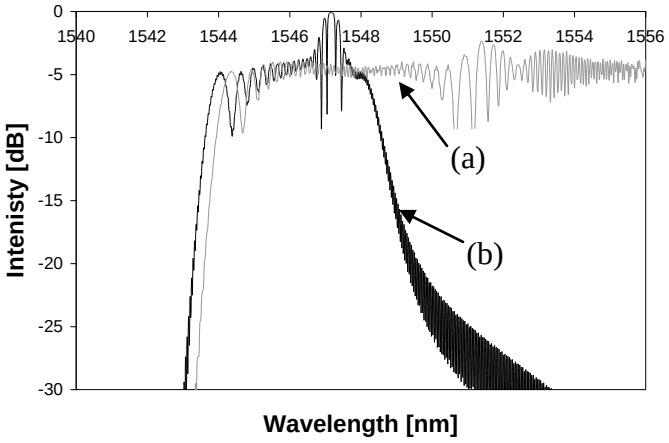

Figure 13. Predictions of reflected spectra from a CFBG sensor located between the repair overply and the parent panel for a scarf-repaired panel under a 1 kN load: (a) reflected spectrum for a repaired panel; (b) reflected spectrum for a panel with a fatigue crack of about 5 mm at the repair/parent panel interface.

7 CONCLUDING REMARKS

The use of CFBG sensors to monitor delamination/disbonding in composite materials is a consequence of the correspondence between the physical location of a non-uniformmity in the strain field experienced by the sensor (as a consequence of damage within the composite) and the perturbation this produces in the reflected spectrum. In many cases, the qualitative interpretation of the perturbations within the spectra due to damage initiation and growth is reasonably straightforward. In addition, predictions of the reflected spectra can be performed to define the location of the damage more accurately and to validate the interpretation of the observations.

8 ACKNOWLEDGEMENTS

The authors would like to thank Mr Peter Haynes for technical support during much of this work.

9 REFERENCES

Stutz, S., Cugnoni, J. & Botsis, J. 2011 Studies of mode I delamination in monotonic and fatigue loading using FBG wavelength multiplexing and numerical analysis. *Composites Science and Technology* **71** 443-449

Capell, T. F., Palaniappan, J., Ogin, S. L., Crocombe, A. D., Reed, G. T., Thorne, A. M., Mohanty, L. & Tjin, S. C. 1997. The use of an embedded chirped fibre Bragg grating sensor to monitor disbond initiation and growth in adhesively bonded composite/metal single lap joints. *Journal of Optics, A: Pure and Applied*, vol 9, pp S40-S44.

Guo, Y. et al. (to be published)

Okabe, Y., Tsuji, R. & Takeda, N., 2004 Application of chirped fibre Bragg grating sensors for identification of crack locations in composites. *Composites A* **35** 59-65

Palaniappan, J., Wang, H., Ogin, S. L., Thorne, A. M., Reed, G. T., Crocombe, A. D. and Tjin, S. C. 2005 Structural health monitoring of bonded composite joints using embedded chirped fibre Bragg gratings *Advanced Composite Letters* **14** 185-92

Palaniappan, J., Ogin, S. L., Thorne, A. M., Reed, G. T., Crocombe, A. D., Capell, T. F. 2008. Disbond growth detection in composite-composite single-lap joints using chirped FBG sensors. *Composites Science and Technology*, *68*(12), 2410-2417.

Rito, R. L., Ogin, S. L., Crocombe, A. D., Capell T. F., Sanderson, A. R., Guo, Y., Tjin, S. C. & Lin B On the use of a CFBG sensor to monitor scarf repairs od composite panels. *Proceedings ETNDT5, Ioaninna, Sept 2011*

Sanderson, A. R., Ogin, S. L., Crocombe, A. D., Gower, M. R L. & Lee, R. J. *Proceedings ICCM18, 18th International Conference on Composite Materials, Korea, Aug 2011*